Available online at www.sciencedirect.com
ScienceDirect
Journal of Organometallic Chemistry 692 (2007) 5501–5507
Journal of Organometallic Chemistry
www.elsevier.com/locate/jorganchem

Note

Azadithiolates cofactor of the iron-only hydrogenase and its PR_3-monosubstituted derivatives: Synthesis, structure, electrochemistry and protonation

Zhen Wang [a], Jian-Hui Liu [a,*], Cheng-Jiang He [a], Shi Jiang [a], Björn Åkermark [b], Li-Cheng Sun [a,c,*]

[a] State Key Laboratory of Fine Chemicals, Dalian University of Technology, Zhongshan Road 158-40, Dalian 116012, PR China
[b] Department of Organic Chemistry, Arrhenius Laboratory, Stockholm University, 10691 Stockholm, Sweden
[c] KTH Chemistry, Organic Chemistry, Royal Institute of Technology, 10044 Stockholm, Sweden

Received 29 March 2007; received in revised form 20 August 2007; accepted 23 August 2007
Available online 29 August 2007

Abstract

The core structure $(\mu\text{-}SCH_2)_2NH[Fe_2(CO)_6]$ (**5**) of Fe-only hydrogenases active site model has been synthesized by the condensation of iron carbonyl sulfides, formaldehyde and silyl protected amine. Its monosubstituted complexes $(\mu\text{-}SCH_2)_2NH[Fe_2(CO)_5PR_3]$ (R = Ph (**6**), Me (**7**)) were accordingly prepared. The coordination configurations of **5** and **6** were characterized by X-ray crystallography. Protonation of complex **7** to form the N-protonated product occurs in an acetonitrile solution upon addition of triflic acid. The redox properties of these model complexes were studied by cyclic voltammetry.

Keywords: Azapropanedithiolate; Phosphine ligand exchange; Iron-only hydrogenase

1. Introduction

Iron hydrogenases (Fe–H_2ase) are highly efficient enzymes that catalyze the reversible reduction of protons to molecular hydrogen [1,2]. Since high-quality structures of the Fe–H_2ase isolated from *Desulfovibrio desulfuricans* and *Clostridium pasteurianum* have been revealed [3,4], the structural and functional models of the Fe-only hydrogenase active site (H-cluster) have turned out to be a fascinating topic due to the potential value of molecular hydrogen as a clean energy carrier. The active site of Fe–H_2ase is comprised of one unusual low-valent diiron disulfide that is linked by a cysteine-ligand to a $[Fe_4S_4]$ cluster, with one bridging carbonyl and additional terminal carbonyl, cyanide and aqua ligands and the non-proteic dithiolate connects to a tether [1,5]. The groups of Pickett, Rauchfuss and Darensbourg have synthesized a number of propyldithiolate diiron analogue and these complexes can produce hydrogen in an electrochemical cell, giving a supply of protons and electrons [6–9]. Certain structural and spectroscopic features of the enzyme have suggested that the structure of this tether is $–SCH_2NHCH_2S–$ (azadithiolate, ADT) or the N-protonated equivalent (see Fig. 1) [10]. In addition, DFT calculations have shown that the amine functionality in this dithiolate is the potential position for protonation, which provides a low energy pathway for hydrogen evolution in the natural system. The protonation at this *N* atom is much more favorable than that with other basic site such as terminal CN or bridging S atom [11]. Although there have been numerous reports regarding the synthesis and electrochemistry of tertiary amine azadithiolate diiron derivatives $(\mu\text{-}SCH_2)_2NR[Fe_2(CO)_6]$ (R = $–CH_3$, 4-$NO_2C_6H_4$, 4-$BrC_6H_4CH_2$, 2-BrC_6H_4,

* Corresponding authors. Address: State Key Laboratory of Fine Chemicals, Dalian University of Technology, Zhongshan Road 158-40, Dalian 116012, PR China. Tel.: +86 411 88993886; fax: +86 411 83072185.
E-mail address: liujh@dlut.edu.cn (J.-H. Liu).

0022-328X/$ - see front matter © 2007 Elsevier B.V. All rights reserved.
doi:10.1016/j.jorganchem.2007.08.026

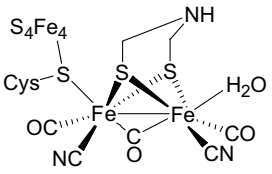

Fig. 1. The active site of Fe-only hydrogenase.

2-$CH_2C_4H_3O$) [12–16], less work has been done to the construction of this parent core structure, i.e., (μ-$SCH_2)_2$-$NH[Fe_2(CO)_6]$. Recently, Rauchfuss et al. reported the first synthesis of this model complex by a three-component condensation starting from iron carbonyl sulfides, formaldehyde, and amines. However, the yield in this reaction was low (37%) and no crystal structure was reported [17]. The synthetic difficulty may probably be attributed to the unstability of the azadithiolate-bridged complex in which the central atom of the chelate is a secondary amine. We decided to assess whether organosilicon reagent could be applied to such reaction as a N-protection reagent. To this end, alkylsilyl chloride was chosen and subjected to aminating with NH_3 or KNH_2, followed by treating with formaldehyde, and finally reacted with Fe–S complex to achieve the condensation. In addition, since the electron-donating characteristics of tertiary phosphine ligands towards the Fe atom are similar to those of CN^- ligands and the complicated protonation on the cyanide nitrogen atom can be avoided, the PR_3-monosubstituted complexes (μ-$SCH_2)_2NH[Fe_2(CO)_5PR_3]$ (R = Ph (**6**), Me (**7**)) were prepared for a study of the influence of phosphine ligands on the coordination structures and the protonation ability. In this paper, we would like to report this modified protocol for the synthesis of (μ-$SCH_2)_2NH[Fe_2(CO)_6]$ (**5**), the conversion to its PR_3-coordinated products as well as their electrochemical properties.

2. Results and discussion

2.1. Synthesis and spectroscopic characterization

Rauchfuss and co-workers have synthesized the core structural molecule (μ-$SCH_2)_2NH[Fe_2(CO)_6]$ (**5**) by the treatment of **3** with a premixed solution of paraformaldehyde and $(NH_4)_2CO_3$ or hexamethylenetetramine in yield of 37% [17]. However, the isolated yield for the target complex is very low (<20%) when we repeated their work. We reasoned that the bridge *N* could be protected to increase the stabilities. Many amine protective groups such as acyl chloride and carbamate are usually removed by treatment with strong base. In contrast, the silyl group can be removed quite easily by treatment with trace acid or in a mild, natural conditions, for instance by using TBAF. Thus, considering the unstability of the Fe_2S_2 skeleton in basic conditions, we choose some silyl reagents as the amino protective groups to achieve the transformation to complex **5**, including triethylsilyl, *t*-butyldimethylsilyl and triisopropylsilyl, which was treated as the alternative amino protective groups. Alkylsilylamine as starting material can react with paraformaldehyde to form the bis(hydromethyl) derivative **2a**–**c** (Scheme 1). Treatment of thiol complex **3** with **2a**–**c** afforded diiron azadithiolates **4a**–**c**. The alkylsilyl groups were simultaneously removed by the excess CF_3COOH existing in the solution to afford **5** in isolated yields of 10% for **1a**, 32% for **1b** and 36% for **1c** (Scheme 1). But we did not obtain the stable nitrogen-protective complex **4a**–**c**, probably due to unstable Si–N bond in the presence of trace acid. Comparing with the isolated yield for **1b** (32%) and **1c** (36%), the yield for **1a** (10%) is quite low. Under the same experimental condition, the unisolated yield of our method is obviously higher than that of Rauchfuss' method.

Monosubstituted complexes (μ-$SCH_2)_2NH[Fe_2(CO)_5L]$ (L = PPh_3 (**6**), PMe_3 (**7**)) were readily prepared in moderate to reasonable yields by treating **5** with PR_3, according to literature procedures (see Scheme 2) [18,19]. Considering the different solubility and coordination ability of the tertiary phosphine, different solvents were used for the individual reactions, with hexane for trimethylphosphine and toluene for triphenylphosphine. While the reaction of **5** with 1 equiv of trimethylphosphine, which has a good coordinated ability, can be controlled at the monosubstituted stage, the reaction to form complex **6** required 2 equiv of PPh_3 in refluxing toluene.

The products **5**–**7** were characterized by IR, ^1H and ^{31}P NMR spectra and elemental analyses. The IR spectra of these three complexes in KBr show three strong CO bands in the region of 1910–2080 cm^{-1}, identical to the carbonyl stretching pattern for terminal CO bonds. In comparison with all carbonyl complex **5**, the average value of the bands for monosubstituted complex **6** and **7** are lowered by 36 and 60 cm^{-1}, respectively.

2.2. Molecular structures of complexes 5 and 6

Single-crystal X-ray diffraction analysis of **5** and **6** (Fig. 2) shows the usual distorted square-pyramidal geometry around the iron centers. The Fe–Fe distances of the two complexes are somewhat shorter than those in the structures of H_2-uptake enzyme from DdHase (*Desulfovibrio desulfuricans*) and H_2-evolving enzyme from CpHase (*Clostridium pasteurianum*) (*ca.* 2.6 Å) [3,4,10], but still in good agreement with the structural data of Fe–Fe bonds (2.49–2.51 Å) found in other diiron azadithiolates complexes [12,15,17]. The CO displacement by one molecule of triphenylphosphine ligand has only a small effect on the Fe–Fe distance [2.519(8) Å in **6**] as compared to that of **5** [2.505(1) Å]. Similar to (μ-$SCH_2)_2NH[Fe_2(CO)_4(CN)_2]$ [17], the N–H of **5** and **6** are all axial as anticipated [11] and the bridging-*N* atoms are of sp^3-hybridization. In the solid state, the nonbonding Fe–H distance between the H atom at the bridging-*N* atom and the nearest Fe atom of **5** is almost consistent with **6** (3.34 and 3.38 Å, respectively), which is significantly longer than that of dicyanide substi-

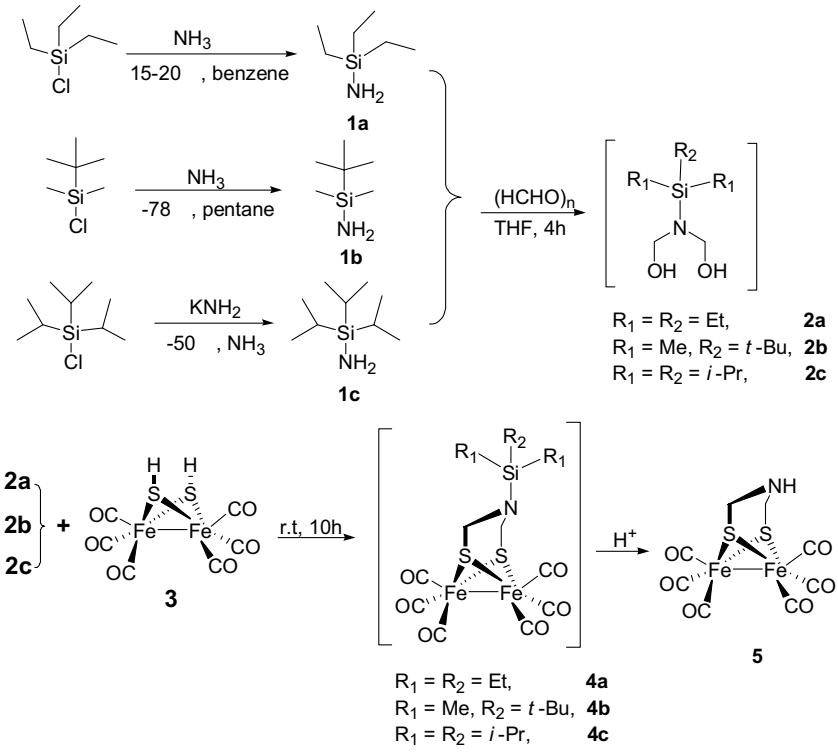

Scheme 1. The synthetic procedure of complexes **5**.

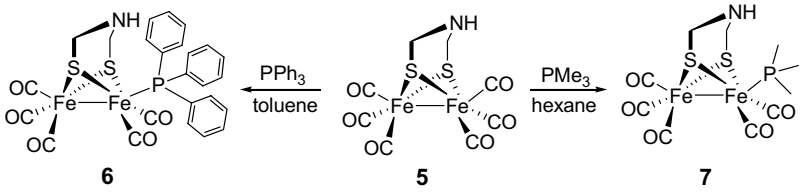

Scheme 2. The transformation of **5** to complexes **6** and **7**.

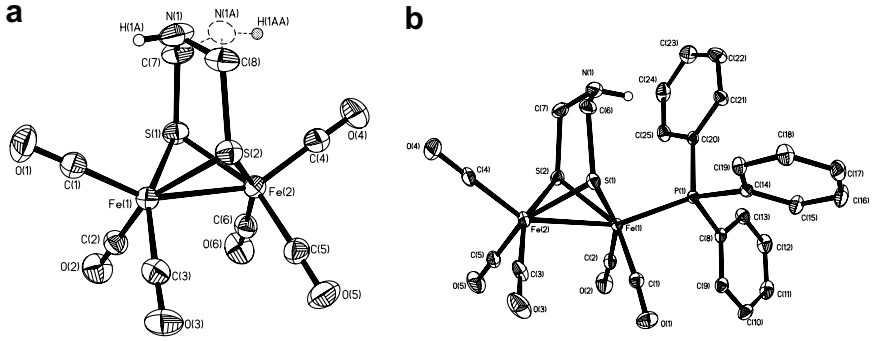

Fig. 2. Molecular structures of **5** (a) and **6** (b), hydrogen atoms omitted for clarity. Selected bond lengths [Å] and angles [°] for complexes **5**: Fe(1)–Fe(2) 2.505(1), Fe–C 1.796(1)–1.803(1), C(8)–N(1)–C(7) 119.7(1), C(7)–N(1A)–C(8) 117.1(1), Sum of angles at N 338.7, 341.1; for complexes **6**: Fe(1)–Fe(2) 2.519 (1), Fe(1)–P(1) 2.244 (1), Fe–C 1.766(2)–1.801(0), C(6)–N(1)–C(7) 116.3(2), Sum of angles at N 336.3.

tuted analogue (3.18 Å) [17]. It is noticeable that the NH group of **6** slants towards the larger electron-density Fe(1) atom. The structural character of **6** may influence hydrogen-evolving processes in the designed molecules. After protonation of **6**, the proton is anticipated to be in proximity to the diiron active site. Triphenylphosphine ligand is coordinated to an apical site on Fe(1) and roughly *trans* to the Fe–Fe bond. Both ^{31}P NMR and X-ray

crystallographic analyses of **6** suggest that one CO displacement by tertiary phosphine in **5** affords only an apical isomer, as shown in Fig. 2b. The angles of C(6)–S(1)–Fe(1) [114.5(1)°] and C(7)–S(2)–Fe(1) [114.8(1)°] in **6** are a little wider than the corresponding angles of C(6)–S(1)–Fe(2) [108.0(1)°] and C(7)–S(2)–Fe(2) [109.1(1)°]. It shows that the six-membered ring of the propanedithiolate in **6** is pushed away from the site occupied by an apical PPh_3 ligand, leading to the lean of the propanedithiolate ring towards the $Fe(CO)_3$ site, as its analogue (μ-pdt) $[Fe_2(CO)_5PPh_3]$ [8].

2.3. Reactions of diiron derivatives with strong acid

Attempts to protonate **5**–**7** were performed in an CH_3CN solution upon addition of triflic acid, but only the complex **7** was observed to be protonated. This result indicates that the basicity of the bridging-*N* atom of the complexes **5** and **6** are too weak to be protonated in the non-aqueous solution. Protonation of **7** was performed with triflic acid in $CHCl_3$ in order to afford an orange precipitate $[(\mu\text{-}SCH_2)_2NH(H)\text{-}\{Fe_2(CO)_5PMe_3\}]^+$ ($[\mathbf{7NHH}]^+$). The IR spectra monitored the whole processes. In CH_3CN solution complex **7** displays three *ν*(CO) bands at 2035, 1965, 1914 cm^{-1}. After 1 equiv of triflic acid was added, the *ν*(CO) bands shifted to higher wavenumber by *ca.*18 cm^{-1}, which is consistent with the observations during the bridging-*N* atom protonation for the related complexes [12,14,15,20]. With the addition of an excess of pyridine to the CH_3CN solution of $[\mathbf{7NHH}]^+$, the *ν*(CO) absorptions shifted to frequencies essentially equivalent to those of parent **7**.

The reversible protonation of **7** and deprotonation of $[\mathbf{7NHH}]^+$ were monitored by the ^1H NMR (Fig. 3). As 5 equiv of triflic acid was added to a solution of **7** in CD_3CN, the signal of the CH_2S at *δ* 3.47 ppm (singlet) shifts to *δ* 3.34 ppm (doublet) and *δ* 3.65 ppm (singlet) shifts to *δ* 3.80 ppm (doublet). Simultaneously a triplet with $^1J_{NH} = 58$ Hz appears at *δ* 6.01, attributing to the proton on the bridge nitrogen of $[\mathbf{7NHH}]^+$ [15]. The two protons of the CH_2S group, which are on the equatorial bonds relative to the 6-membered ring [Fe(1)–S(2)–C(7)–N(1)–C(6)–S(1), Fig. 2] and *cis* to the proton of the NH group, should display higher resonances than those on the vertical bonds and *trans* to the proton of the NH group. All observations in the ^1H NMR spectra are consistent with the protonation of the bridging-*N* atom. No peaks at $\delta < 0$ exist in the ^1H NMR were observed, showing that the protonation occurred on the *N* atom rather than to form μ-H complex at the Fe–Fe site. Upon addition of an excess of pyridine to the solution of $[\mathbf{7NHH}]^+$ in CD_3CN, a triplet with $^1J_{NH} = 67$ Hz emerges at *δ* 13.56, and at the same time all signals move back to the original. The newly-formed triplet in the low field region is assigned to the NH of protonated pyridine [21]. From Fig. 3c, we can see that the deprotonation of $[\mathbf{7NHH}]^+$ occurs instantly to afford **7** and pyridinium triflate in the presence of pyridine.

2.4. Cyclic voltammograms of model complexes 5–7 and [7NHH]$^+$

Electrochemistry of model complexes were studied to evaluate their redox properties. The electrochemical data are presented in Fig. 4. Complexes **5**–**7** each display one irreversible oxidation peak and one irreversible reduction peak. Compared with the electrochemical data of the azadithiolat diiron complexes and other analogous [13,14,21], the oxidation peaks at the range of 0.1–0.6 V versus Fc/Fc^+ are assigned to the $Fe^{(I)}Fe^{(I)}/Fe^{(II)}Fe^{(I)}$ process. The reductive peaks at the range of −1.5 to −1.9 V are ascribed to the one-electron process $Fe^{(I)}Fe^{(I)}/Fe^{(0)}Fe^{(I)}$. Compared to the $(\mu\text{-pdt})Fe_2(CO)_6$ ($pdt = SCH_2CH_2CH_2S$) ($E_{red} = -1.67$ V versus Fc/Fc^+) [14], the reductive potential of **5** (−1.58 V) was less negative, which is close to the value of the tertiary amine azadithiolate diiron derivatives

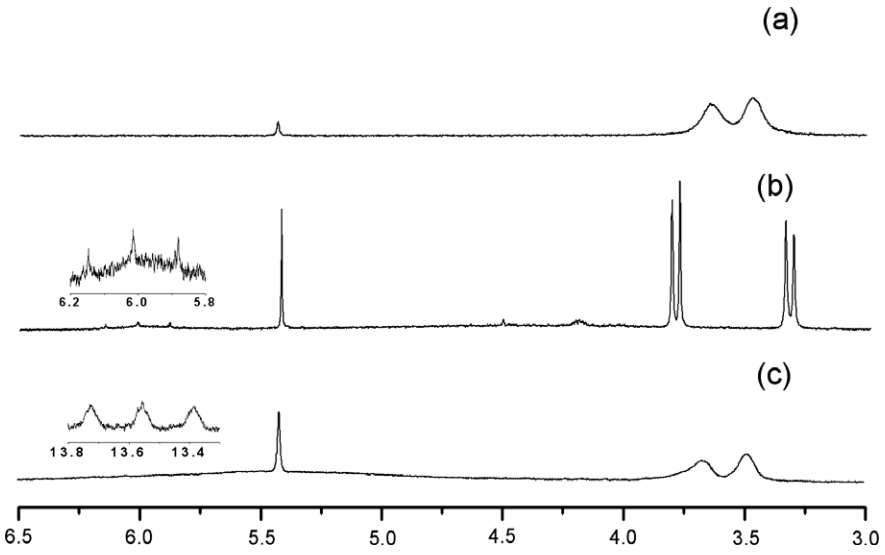

Fig. 3. ^1H NMR spectra of (a) **7** in CD_3CN, (b) $[\mathbf{7NHH}]^+$ (5 equiv CF_3SO_3H in CD_3CN), (c) $[\mathbf{7NHH}]^+$ + 6 equiv pyridine in CD_3CN.

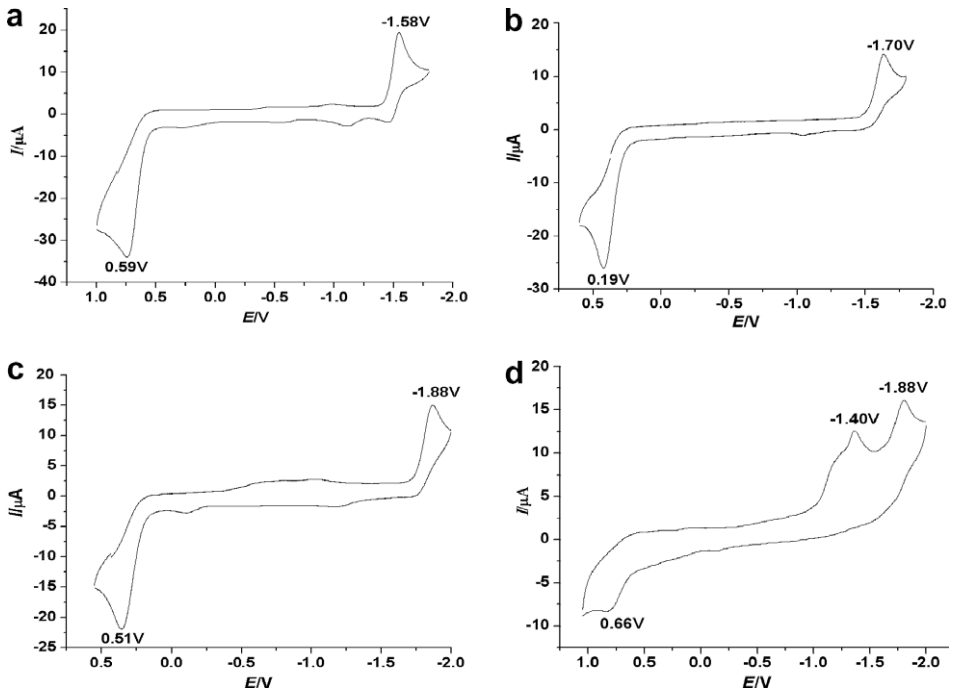

Fig. 4. Cyclic voltammograms of **5** (a), **6** (b), **7**(c) and [**7NHH**]$^+$(d), 1.0 mmol in 0.05**M** [*n*-Bu_4NPF_6]/CH_3CN at a scan rate of 100 mV s^{-1}. Potentials are vs. Fc/Fc^+.

$(\mu\text{-}SCH_2)_2NR[Fe_2(CO)_6]$ (R = 4-$NH_2C_6H_4$ (−1.58 V), 4-Br $C_6H_4CH_2$ (−1.56 V), 2-$CH_2C_4H_3O$ (−1.55 V)) [13,14,16]. The replacement of one CO for one PR_3 leads to a negative shift of the reduction potential by *ca*. 0.12 and 0.3 V for **6** and **7**, respectively, as compared to that of the all-carbonyl parent complex **5**. The reduction potential for **6** is obviously less negative than that for complex **7** by 180 mV, indicative of a considerable influence of different phosphine ligands on the redox properties of the iron atoms of Fe-only hydrogenase-active-site model complexes. As addition of 2 equiv of triflic acid to the CH_3CN solution of **7**, the cyclic voltammogram of [**7NHH**]$^+$ is observed. The first reductive peak is shifted by 480 mV towards more positive potential compared to that of complex **7**, which is a result of the fact that [**7NHH**]$^+$ carries a proton, and this reductive peak is corresponding to a one-electron reduction of the protonated complex to [7NHH]$^+$ [14].

3. Conclusions

In summary, the desired diiron azadithiolate complexes $(\mu\text{-}SCH_2)_2NH[Fe_2(CO)_6]$ (**5**) was synthesized starting from the alkylsilyl-protected material, and its PR_3-monosubstituted derivatives $(\mu\text{-}SCH_2)_2NH[Fe_2(CO)_5PR_3]$ (R = Ph (**6**), Me (**7**)) were also obtained. The crystal structure of the complex **6** showed that the N–H bond is in axial position and close to the higher electron-density Fe atom. This may indicate that the hydrogen on the bridged-*N* atom plays a very important role in the catalyzing the reversible reaction of protons and electrons to molecular hydrogen. The result of the protonation of **5**–**7** showed that only by coordinating of a strong electron-donating ligand, the bridging nitrogen atom can be protonated and assists the formation of the H–H bond to produce molecular hydrogen during the catalytic cycle.

4. Experimental

4.1. Reagents and instruments

All manipulations related to organometallic complexes were performed under dry, oxygen-free nitrogen gas with standard Schlenk techniques. All solvents were purified according to standard methods. Commercially available chemicals, including paraformaldehyde, *t*-butyldimethylsilyl chloride, triethylsilyl chloride, triisopropylsilyl chloride, tertiary phosphanes and $Fe(CO)_5$, were used without further purification. The reagent $LiEt_3BH$ was purchased from Aldrich. Starting compounds triethylsilylamine (**1a**) [22], *t*-butyldimethylsilylamine (**1b**) [23], triisopropylsilylamine (**1c**) [24], $(\mu\text{-}S)_2[Fe_2(CO)_6]$, $(\mu\text{-}HS)_2[Fe_2(CO)_6]$ (**3**) were prepared according to literature methods [25,26]. All other reagents were used as purchased without further purification. ^1H and ^{31}P NMR spectra were recorded on a Varian INOVA 400 spectrometer. IR spectra were recorded from KBr pellets with a JASCO FT/IR430. Elemental analyses were performed with a Thermoquest-Flash EA 1112 elemental analyzer.

4.2. Procedures

4.2.1. $(\mu\text{-}SCH_2)_2NH\ [Fe_2(CO)_6]$ (5)

A mixture of triethylsilylamine (393 mg, 3.00 mmol), paraformaldehyde (304 mg, 0.01 mol) and THF (25 mL)

was stirred for *ca.* 4 h. Then it was treated with a THF solution (25 mL) of **3** (0.59 mmol) and stirred for further 10 h. After removing THF under vacuum, the crude product was purified by flash chromatography on silica gel eluting with hexane/CH_2Cl_2 (8:1) to give **5** as a red solid (24 mg, 10%). The crystal suitable for X-ray analysis was obtained from a solution of hexane at 2 °C. ^{1}H NMR ($CDCl_3$) δ 3.56 (s, 4H, NCH_2S), IR (KBr, νCO): $\nu = 2073$, 2031, 1994 cm^{-1}. Anal. Calc. for $C_8H_5Fe_2NO_6S_2$: C, 24.83; H, 1.30; N, 3.62. Found: C, 24.79; H, 1.31; N, 3.65%.

The synthetic procedure of complexes **5** started from *t*-butyldimethylsilylamine (**1b**) and triisopropylsilylamine (**1c**) is similar to that of triethylsilylamine (**1a**). The yield is, respectively, 32% for **1b** and 36% for **1c**.

4.2.2. (μ-$SCH_2)_2NH$ [$Fe_2(CO)_5PPh_3$] (6)

To the red solution of hexacarbonyldiiron dithiolate **5** (50 mg, 0.129 mmol) in toluene (10 mL) was added triphenylphosphine (135 mg, 0.258 mmol). The reaction mixture was refluxed for 4 h and the color turned to dark red. After the solvent was removed in vacuum, the crude product was purified by column chromatography on silica gel with hexane/CH_2Cl_2 (4:1) as eluent to give **6** as red solid (32 mg, 40%). The crystal suitable for X-ray analysis was obtained from a solution of hexane/CH_2Cl_2 (10/1) at 2 °C. ^{1}H NMR ($CDCl_3$) δ 7.72 (s, 9H, Ph), 7.46 (s, 6H, Ph), 3.18 (s, 4H, SCH_2N), ^{31}P NMR ($CDCl_3$) δ 65.52; IR (KBr, νCO): $\nu = 2035$, 1985, 1974 cm^{-1}. Anal. Calc. for $C_{25}H_{20}Fe_2NO_5PS_2$: C, 48.33; H, 3.25; N, 2.25. Found: C, 48.91; H 3.24; N 2.22%.

4.2.3. (μ-$SCH_2)_2NH$ [$Fe_2(CO)_5PMe_3$] (7)

To the red solution of hexacarbonyldiiron dithiolate **5** (50 mg, 0.129 mmol) in hexane (10 mL) was added trimethylphosphine (10 mg, 0.129 mmol). The reaction mixture was refluxed for 1 h and the color turned to dark red. After the solvent was removed in vacuum, the crude product was purified by column chromatography on silica gel with hexane/CH_2Cl_2 (3:1) as eluent to give **7** as a red solid (32 mg, 40%). ^{1}H NMR ($CNCD_3$) 3.65 (s, 2H, SCH_2N), 3.47(s, 2H, SCH_2N), 1.48(d, $J_{PH} = 9.6$ Hz, 9H, CH_3) ^{31}P NMR ($CDCl_3$) δ 26.46; IR (KBr, νCO): $\nu = 2035$, 1965, 1914 cm^{-1}. $C_{10}H_{14}Fe_2NO_5PS_2$ (435.02): Anal. Calc. C, 27.61, H, 3.24, N, 3.22. Found: C 27.21, H 3.24, N 3.19%.

4.3. Crystal structure determinations of complexes 5 and 6

The single crystal X-ray diffraction data were collected with a Siemens Smart CCD diffractometer equipped with graphite monochromated Mo Kα radiation ($\lambda = 0.71073$ Á) for **5** and with a Rigaku R-axis rapid-IP equipped with graphite monochromated Mo Kα radiation ($\lambda = 0.71073$ Á) for **6**. Complete crystal data and parameters for data collection and refinement are listed in Table 1. The structure was solved by direct methods and subsequent difference Fourier syntheses, and refined on F_2 against full-matrix least-squares methods by using the SHELXTL-97 program package. All non-hydrogen atoms were refined anisotropically. The hydrogen atoms of the NH group in **5** and **6** were located from Fourier difference maps and the other H-atoms located by geometrical calculation, but their positions and thermal parameters were fixed during the structure refinement.

Table 1
Crystallographic data and processing parameters for complexes **5** and **6**

	5	**6**
Empirical formula	$C_8H_5Fe_2NO_6S_2$	$C_{25}H_{20}Fe_2NO_5PS_2$
Formula weight	386.95	621.22
Crystal system	Monoclinic	Monoclinic
Space group	*P*2(1)/*n*	*P*2(1)/*c*
a (Å)	7.8127(4)	9.1382(18)
b (Å)	15.1218(9)	17.286(4)
c (Å)	11.7395(5)	16.651(3)
α (°)	90.00	90.00
β (°)	99.902(2)	102.44(3)
γ (°)	90.00	90.00
Volume (Å^3)	1366.27(12)	2568.4(9)
Z	4	32
D_{calc} (Mg/m^3)	1.881	1.606
F(000)	768	1264
Crystal size (mm)	0.35 × 0.22 × 0.2	0.3 × 0.25 × 0.22
Range for data collection (°)	2.22–25.08	1.72–27.43
Reflections collected	2400	5538
Independent reflections (R_{int})	2034 (0.0219)	4350 (0.0416)
Completeness to θ	25.08°, 98.9%	27.43°, 94.5%
Data/restraints/parameters	2400/2/188	5538/0/329
Goodness-of-fit on F^2	1.068	0.980
Final *R* indices ($I > 2\sigma(I)$)	$R_1 = 0.0440$	$R_1 = 0.0272$
	$wR_2 = 0.0892$	$wR_2 = 0.0655$
R indices (all data)	$R_1 = 0.0573$	$R_1 = 0.0412$
	$wR_2 = 0.0987$	$wR_2 = 0.0773$
Largest difference in peak and hole (e Å^{-3})	0.457 and −0.389	0.507 and −0.400

4.4. Crystal data for 5 and 6

Crystallographic data and processing parameters for complexes **5** and **6** are given in Table 1.

4.5. Electrochemistry

A solution of 0.05 M of *n*-Bu_4NPF_6 (Fluka, electrochemical grade) in CH_3CN was used as electrolyte, which was degassed by bubbling with dry argon for 10 min before measurement. Electrochemical measurements were recorded using a BAS-100W electrochemical potentiostat at a scan rate of 100 mV/s. Cyclic voltammograms were obtained in a three-electrode cell under argon. The working electrode was a glassy carbon disc (diameter 3 mm) successively polished with aqueous alumina powder slurry for 10 min. The reference electrode was a non-aqueous Ag/Ag^+ electrode (0.01 m $AgNO_3$ in CH_3CN) and the auxiliary electrode was a platinum wire.

5. Supplementary material

CCDC 239490 and 244941 contain the supplementary crystallographic data for (μ-$SCH_2)_2NH[Fe_2(CO)_6]$ and

$(\mu\text{-}SCH_2)_2NH[Fe_2(CO)_5PPh_3]$. These data can be obtained free of charge via http://www.ccdc.cam.ac.uk/conts/retrieving.html, or from the Cambridge Crystallographic Data Centre, 12 Union Road, Cambridge CB2 1EZ, UK; fax: (+44) 1223 336 033; or e-mail: deposit@ccdc.cam.ac.uk.

Acknowledgements

We are grateful to the Ministry of Science and Technology of China and the Chinese National Natural Science Foundation (Grant No. 20471013, 20633020 and 20672017), the Swedish Energy Agency, the *K&A* Wallenberg Foundation, the Program of Introducing Talents of discipline to Universities, and the Swedish Research Council for financial supports of this work.

References

[1] Y. Nicolet, B.J. Lemon, J.C. Fontecilla-Camps, J.W. Peters, Trends Biochem. Sci. 25 (2000) 138.
[2] M.Y. Darensbourg, E.J. Lyon, J.J. Smee, Coord. Chem. Rev. 206–207 (2000) 533.
[3] J.W. Peters, W.N. Lanzilotta, B.J. Lemon, L.C. Seefeldt, Science 282 (1998) 1853.
[4] Y. Nicolet, C. Piras, P. Legrand, C.E. Hatchikian, J.C. Fontecilla-Camps, Structure 7 (1999) 3.
[5] M. Frey, ChemBioChem 3 (2002) 153.
[6] C. Tard, X.-M. Liu, S.K. Ibrahim, M. Bruschi, L.D. Gioia, S.C. Davies, X. Yang, L.-S. Wang, G. Sawers, C.J. Pickett, Nature 433 (2005) 610.
[7] (a) F. Gloaguen, J.D. Lawrence, T.B. Rauchfuss, J. Am. Chem. Soc. 123 (2001) 9476;
(b) F. Gloaguen, J.D. Lawrence, T.B. Rauchfuss, M. Benard, M.M. Rohmer, Inorg. Chem. 41 (2002) 6573.
[8] P. Li, M. Wang, C.-J. He, G.-H. Li, X.-Y. Liu, C.-N. Chen, B. Åkermark, L.-C. Sun, Eur. J. Inorg. Chem. (2005) 2506.
[9] R. Mejia-Rodriguez, D. Chong, J.H. Reibenspies, M.P. Soriaga, M.Y. Darensbourg, J. Am. Chem. Soc. 126 (2004) 12004.
[10] Y. Nicolet, A.L. Lacey, X. VernTde, V.M. Fernandez, E.C. Hatchikian, J.C. Fontecilla-Camps, J. Am. Chem. Soc. 123 (2001) 1596.
[11] (a) H.J. Fan, M.B. Hall, J. Am. Chem. Soc. 123 (2001) 3828;
(b) Z.P. Liu, P. Hu, J. Am. Chem. Soc. 124 (2002) 5175;
(c) Z.-P. Liu, P. Hu, J. Chem. Phys. 117 (2002) 8177.
[12] J.D. Lawrence, H.-X. Li, T.B. Rauchfuss, M. B Tnard, M. Rohmer, Angew. Chem., Int. Ed. 40 (2001) 1768.
[13] T.-B. Liu, M. Wang, Z. Shi, H.-G. Cui, W.-B. Dong, J.-S. Chen, B. Åkermark, L.-C. Sun, Chem. Eur. J. 10 (2004) 4474.
[14] S. Ott, M. Kritikos, B. Åkermark, L.-C. Sun, R. Lomoth, Angew. Chem., Int. Ed. 43 (2004) 1006.
[15] F. Wang, M. Wang, X. Liu, K. Jin, W. Dong, G. Li, B. Åkermark, L. Sun, Chem. Commun. 25 (2005) 3221.
[16] S. Jiang, J.-H. Liu, L.-C. Sun, Inorg. Chem. Commun. 9 (2006) 290.
[17] H.-X. Li, T.B. Rauchfuss, J. Am. Chem. Soc. 124 (2002) 726.
[18] J.A. de Beer, R.J. Haines, J. Organomet. Chem. 37 (1972) 173.
[19] J.A. de Beer, R.J. Haines, J. Organomet. Chem. 36 (1972) 297.
[20] W.-M. Gao, J.-H. Liu, C.-B. Ma, L.-H. Weng, K. Jin, C.-N. Chen, B. Åkermark, L. Sun, Inorg. Chim. Acta 359 (2006) 1070.
[21] K.S. Mohamed, D.K. Padma, Spectrochim. Acta 41A (1985) 725.
[22] D.M. Choquetbt, M.J. Timm, J.L. Hobbs, M.M. Rahim, K.J. Ahmed, R.P. Planalp, Organometallics 11 (1992) 529.
[23] R. West, P. Boudjouk, J. Am. Chem. Soc. 95 (1973) 3983.
[24] H.-J. Goetze, B. Bartylla, M. Ismeier, Spectrochim. Acta Part A 49 (1993) 497.
[25] D. Seyferth, R.S. Henderson, J. Organomet. Chem. 218 (1981) C34.
[26] D. Seyferth, R.S. Henderson, L.-C. Song, Organometallics 1 (1982) 125.